Draft version July 25, 2014
Preprint typeset using LaTeX style emulateapj v. 04/17/13

THE DEPENDENCE OF SPIRAL DISK MORPHOLOGY ON THE STAR FORMATION-STELLAR MASS RELATION

Kyle Willett[1], Kevin Schawinski[2], etc.

Draft version July 25, 2014

ABSTRACT

We measure the mass-star formation relation in disk galaxies at $z < 0.05$, using Galaxy Zoo morphologies to examine different populations of spirals as classified by their kiloparsec-scale structure. We examine the number of arms, their average pitch angle, and the presence of a galactic bar, and show that both the slope and dispersion of the SFR-$M_\star$ relation is constant when varying all the above parameters. We interpret this as evidence that the spiral arms, which are imperfect reflections of the galaxy's current gravitational potential, are either fully independent of the basic quenching relation or are completely overwhelmed by the combination of outflows and feedback. The arrangement of the star formation can be changed (as demonstrated by the filling factor of the disk), but the system *as a whole* regulates itself. We also show that mergers (both major and minor), which represent the strongest conditions for increases in star formation at a constant mass, only drive the galaxies off the main relation by ~ 0.3 dex; this is a significant reduction over merging systems at $z > 1$.

Subject headings: galaxies:mergers

1. INTRODUCTION

Observations at a range of redshifts have established that the star formation rate (SFR) of a galaxy is strongly correlated to its stellar mass ($M_\star$). This 'main sequence' of star formation is nearly linear and at least at low redshift, has remarkably small scatter (refs). Recent observations of star-forming galaxies at high redshifts show that this main sequence remains out to high redshift with the normalisation of the main sequence shifting up so that galaxies of the same $M_\star$ have a higher SFR at high redshift (refs). The main sequence has been interpreted by Bouché et al. (2010) and Lilly et al. (2013) as the result of the balancing of inflows of cosmological gas and outflows due the feedback. Galaxies self-regulate to remain in a state of homeostasis as they convert baryons from gas to stars.

As star-forming galaxies exhibit a wide range of physical appearances in optical images, we can ask the natural question of whether the specifics of this physical appearance, and its underlying dynamical processes, have any effect on this homeostasis and therefore the galaxy's location relative to the SFR-$M_\star$ relation. If the details of a galaxy's physical appearance are correlated with position relative to the main sequence, then the dynamical processes that give rise to them – such as bar formation and spiral arm pitch angle – are a fundamental aspect of the galaxy's regulatory mechanism. If on the other hand they are not correlated, then there are two options: either they are simply not relevant, or the regulatory mechanism overcomes them in virtually all circumstances. This would speak to the strength of the regulator.

Discuss (**Kevin**) seminal work of Peng et al. (2010, 2012, 2014); Peng & Maiolino (2014) on gas regulator model and how mass/environment drive galaxy evolution.

In this paper, we use the Sloan Digital Sky Survey (York et al. 2000; Strauss et al. 2002; Abazajian et al. 2009) in combination with the largest database of visual classifications of galaxy structure and morphology ever assembled from the Galaxy Zoo citizen science projects (Lintott et al. 2008, 2011; Willett et al. 2013) to test whether galaxy structure affects their star formation properties.

2. DATA

Data for all galaxies in this paper comes from optical observations in the SDSS DR7. The morphological data is drawn from citizen science classifications in Galaxy Zoo. Merging pairs of galaxies are taken from the catalog of Darg et al. (2010a), all of which lie in the redshift range $0.005 < z < 0.1$. Post-merger spheroidal galaxies without an obvious, separated companion (Carpineti et al. 2012) are specifically excluded from the sample. Detailed classifications of disk morphologies (arm pitch angle, number of spiral arms, presence of a galactic bar) are taken from the Galaxy Zoo 2 (GZ2) catalog (Willett et al. 2013).

Spiral galaxies are selected according to the following thresholds in the spectroscopic GZ2 sample, where p is the debiased vote fraction and N the weighted number of total votes: $p_{\mathrm{features/disk}} > 0.430$, $p_{\mathrm{not\ edgeon}} > 0.715$, $p_{\mathrm{spiral}} > 0.619$, and $N_{\mathrm{spiral}} > 20$. We identify sub-classes of spiral structure using the morphology flags as given in the GZ2 catalog; these are designed to be conservative cuts, including only robust examples of each morphological class.

Stellar masses and star formation rates are computed from optical diagnostics and taken from the MPA-JHU catalogue (Kauffmann et al. 2003a; Brinchmann et al. 2004). We use updated masses and activity classifications from the DR7 database.[3] We separate star-forming galaxies from other emission-line galaxies using the stan-

[1] School of Physics and Astronomy, University of Minnesota, Minneapolis, MN 55455, USA
[2] Institute for Astronomy, Department of Physics, ETH Zürich, Wolfgang-Pauli-Strasse 16, CH-8093, Zürich, Switzerland

[3] http://home.strw.leidenuniv.nl/~jarle/SDSS/

TABLE 1
Basic properties of the $M_\star - SFR$ linear fit for GZ2 star-forming galaxies.

Sample	N	α	β	σ_α	σ_β
SF galaxies	52685	0.73	−7.19	5.27×10^{-6}	5.18×10^{-4}
1 arm	39	0.66	−6.31	5.11×10^{-3}	5.14×10^{-1}
2 arms	2914	0.79	−7.74	1.11×10^{-4}	1.14×10^{-2}
3 arms	89	0.57	−5.47	4.17×10^{-3}	4.49×10^{-1}
4 arms	9	0.35	−3.29	9.18×10^{-2}	9.58×10^{0}
5+ arms	9	0.64	−6.88	7.20×10^{-2}	6.91×10^{0}
can't tell	40	0.69	−7.10	1.06×10^{-2}	1.04×10^{0}
tight arms	308	0.73	−7.26	1.68×10^{-3}	1.75×10^{-1}
medium arms	44	0.80	−7.83	5.23×10^{-3}	5.37×10^{-1}
loose arms	470	0.74	−7.14	5.16×10^{-3}	5.18×10^{-2}
barred	4473	0.76	−7.54	7.60×10^{-5}	7.57×10^{-3}
unbarred	11593	0.70	−6.92	2.65×10^{-5}	2.66×10^{-3}
merger	2978	–	−7.91	–	4.40×10^{-4}

Note. — Parameters are according to Equation 1.

dard BPT classification (Baldwin et al. 1981) below the Kauffmann et al. (2003b) demarcation. Galaxies with low signal-to-noise ratio ($S/N > 3$) galaxies are removed. For both $M_\star$ and SFR, we use median values extracted from the PDF.

The total sample analyzed contains 52,685 star-forming galaxies. These are selected from the GZ2 spectroscopic sample with $z < 0.1$, $M_r < -19.5$, and classified as actively star-forming (BPT= 1) from the MPA-JHU emission line measurements. The average color for the star-forming galaxies is relatively blue, with $(u - r) = 1.7 \pm 0.6$. Subsets of the star-forming galaxies are listed in Table 1.

To analyze the $M_\star - SFR$ relationship, we apply a simple linear model for the total sample and subsamples. We apply a least-squares fit where the data are weighted by the uncertainty in SFR (computed as the mean difference in the 16th and 84th percentiles from the MPA-JHU PDFs). The data are then fit to:

$$\log(SFR) = \alpha(\log[M_\star/M_\odot]) + \beta \qquad [M_\odot/yr] \qquad (1)$$

where α and β represent the slope and offset, respectively. Values of the fits for each subample are given in Table 1; we also provide the formal uncertainties σ_α and σ_β in each parameter from the covariance matrix.

Come up with a more sensible measure of the uncertainty - the formal covariance elements clearly don't represent the dispersion in the main sequence. Interquartile range?

3. RESULTS

We analyze the dependence of the star-forming main sequence for three different sets of disk galaxies: splitting the sample by the observed number (multiplicity) of spiral arms, the relative pitch angle (tightness or winding) of the spiral arms, and the presence of a galactic bar. Both spiral arms and galactic bars can have significant effects on the local properties of a galaxy. Dynamical effects compress gas and trigger recent star formation within spiral arms, while longer galactic bars have redder colors and less star formation than the rest of the disk (Hoyle et al. 2011). We examine whether these kpc-scale effects can be seen long-term in the galaxy's SFR-mass relationship.

For the control sample, we plot in Figures 1-4 the underlying star-forming main sequence relation for star-forming disks as measured in a sample of local SDSS galaxies. As demonstrated in previous papers, there is a fairly tight correlation between $M_\star$ and SFR, with galaxies in the process of quenching lowering their SFR and falling below the trend. The relationship extends over at least 4 orders of magnitude in both $M_\star$ and SFR.

Figure 1 overplots the $M_\star - SFR$ relationship for disk galaxies separated by their arm multiplicity. The GZ2 data separates disk galaxies with visible spiral arms into categories of 1, 2, 3, 4, or more than four spiral arms; there is also an additional option if the number of spiral arms cannot be accurately determined. There are a total of 14,179 galaxies with flags for arm multiplicity (indicating a high level of agreement among classifiers) in the GZ2 data. Of those, two-armed spirals are by far the most common, comprising 85% of the total. This is also the only multiplicity for which significant numbers of galaxies at $M_\star < 10^9\ M_\odot$ are detected.

The fit to the star-forming main sequence for two-armed spirals tighly follows that of that for all spiral galaxies, with both the slope and offset of the linear fits completely consistent with each other (Table 1). Similarly, the fits for 3, 4, and 5+-armed spirals are also consistent with the main relation (although all three have much lower numbers which affect the quality of the fit).

1-armed spirals present an interesting case, with the majority of the population lying slightly above the fit to all star-forming spirals. This is consistent with the work of Casteels et al. (2013), who showed that 1-armed spirals in GZ2 are robust indicators of close interactions at projected distances of $r_p < 50\ h^{-1}$ kpc. The underlying reason is that many "1-armed spirals" are in fact caused by bridges or tidal tails from interactions with a nearby companion; we discuss the likely role of merging/interacting galaxies in Figure 4.

Finally, galaxies with an uncertain number of spiral arms (although also with relatively low numbers) fall slightly below the mean star-forming main sequence relation. We conjecture that this is a consequence of galaxies that have likely already begun the process of quenching. As a result, the star-formation rate is depleted and the contrast of spiral arms against the rest of the disk (which for visual identification is at least in part dependent on bright knots of recent star formation) makes the multiplicity more difficult to identify. *(**Kevin**: check colors of these galaxies and see if they lie in the green valley? Would be a nice test to see if they're consistent with the red herring model.)*

The pitch angle of the spiral arms also has no significant change on the star-forming main sequence relation (Figure 2). We separate galaxies by their relative pitch angles (defined as "tight", "medium", and "loose"); the pitch angle is typically used as one of the primary drivers for separating galaxies along the Hubble tuning fork. Willett et al. (2013) show, however, that pitch angle only weakly correlates with Hubble type from expert visual classifications, and that the bulge-to-disk ratio is a more important driver. All three categories correlate tightly with spiral galaxies in general; we note that the small deviation above the main sequence for loosely-wound galaxies is also consistent with Casteels et al. (2013), who show that this morphology also correlates with close pairs and

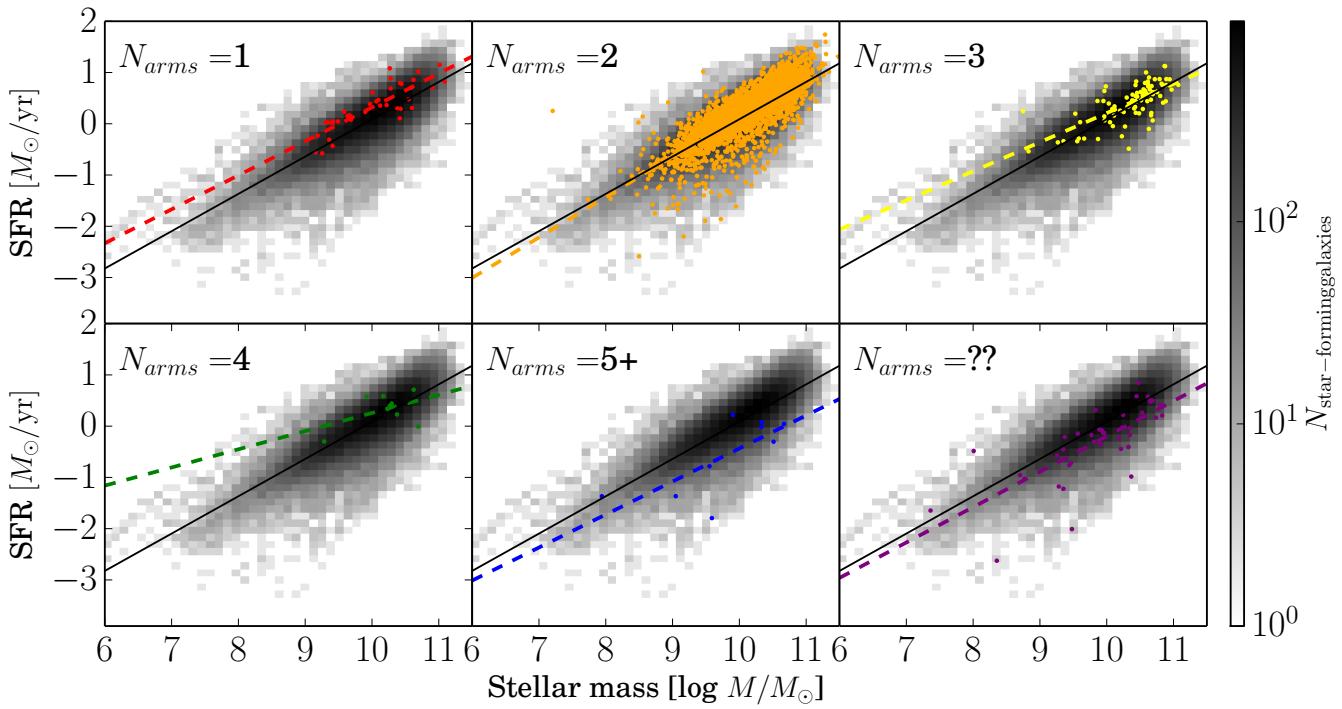

FIG. 1.— Stellar mass vs. star formation rate; grayscale colors are the distribution of all star-forming galaxies from the MPA-JHU catalog. Colored points in each panel show spiral galaxies with "tight", "medium", and "loose" spiral arms as identified by morphology flags in GZ2. Dotted lines show the weighted least-squares linear fit to the population as split by pitch angle; the solid line is the fit to all star-forming galaxies.

interactions.

It should also be noted that the galaxies in GZ2 flagged as a function of pitch angle are not representative of the true vote distribution. The raw numbers in Figure 2 suggest that most spiral galaxies are either tightly or loosely wound. In fact, the plurality classification for most galaxies is for medium-winding; the spread in votes is typically large, though, and so users rarely agree on the medium option at the 80% level which sets the flag. Plotting the same star-forming main sequence diagram as a function of p_{medium}, which more accurately tracks the pitch angle distribution, also closely follows the main star-forming main sequence.

Finally, we examine the effect of a large-scale galactic bar on the star-forming main sequence. This sample is significantly larger than those including spiral arm morphology, since the classification is at a higher level in the GZ2 tree and has only two choices; this results in a higher percentage of consensus classifications that set the flag. Figure 3 shows the star-forming main sequence for both barred and unbarred galaxies. Although the fraction of barred galaxies potentially varies as a function of stellar mass (Masters et al. 2011), both the linear fits and ranges of the sub-populations are consistent with all star-forming galaxies. In other words, the presence of a bar does not affect the galaxy's position on the star-forming main sequence.

4. DISCUSSION

There is no significant difference between any of the morphological categories explored. Statistical test for how "not different" the categories are.

This is interpreted as evidence that the regulation of the star formation rate is independent of the details of galactic structure as traced by the dynamics of the spiral arms.

Conditional statements: if the situation above is true, then the following must apply.

Bar results are in rough agreement with the mass-dependent trends seen in Ellison et al. (2011); strong difference is only seen at $M_\star > 10^7\ M_\odot$, which is at the very upper end of our range.

Point that has not been made before; self-regulated systems where you can move parts around, but the total amount must be conserved. Process as a result cannot be simply regulated locally - the whole system must know about the rate of regulation. What does this say about the minimum lifetime of the features as a dynamical timescale τ_{dyn}?

The biggest forcing we can think of for the system is a major merger. Even that doesn't push it too far off the main sequence, indicating short timescales and higher levels of feedback. Figure 4 shows the relation for systems of merging galaxies (Darg et al. 2010a). For these systems, there is a small increase in the offset of the $M_\star - SFR$ relation, but none in the slope. The difference is ~ 0.2 dex, an increase of only $\sim 70\%$ in star-formation rate for a given mass. There are a very small number of galaxies whose star formation rates lie more than an order of magnitude above the standard relation, but the numbers are too small to make a significant contribution to the SFR density of the local Universe.

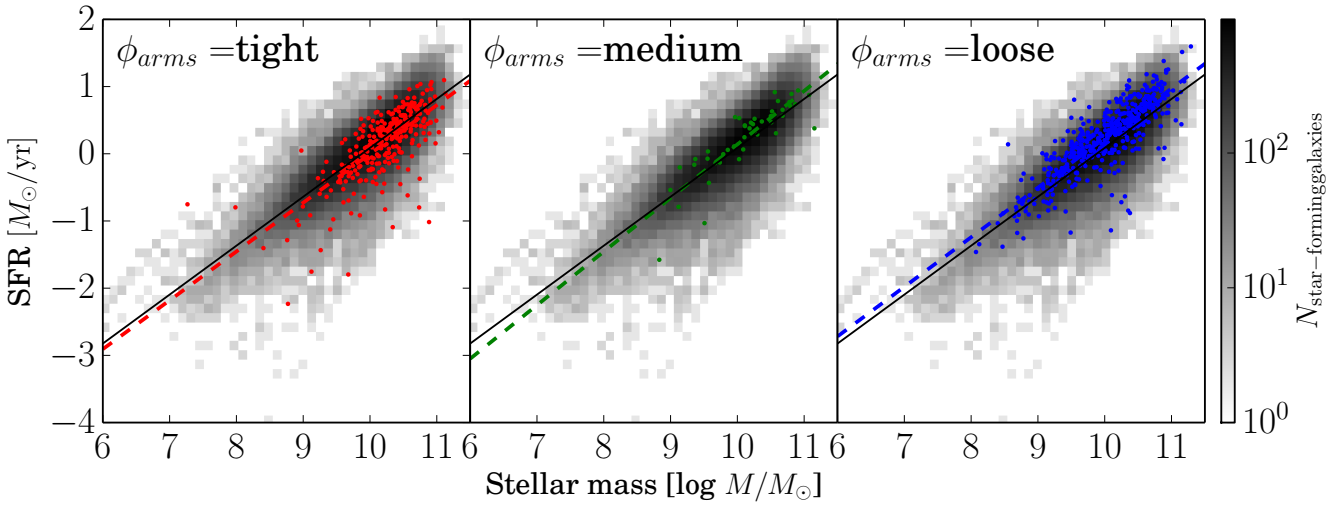

FIG. 2.— Stellar mass vs. star formation rate; grayscale colors are the distribution of all star-forming galaxies as in Figure 1. From left to right: red, green, and blue points spiral galaxies with "tight", "medium", and "loose" spiral arms as identified by morphology flags in GZ2. Dotted lines show the weighted least-squares linear fit to the population as split by pitch angle; the solid line is the fit to all star-forming galaxies.

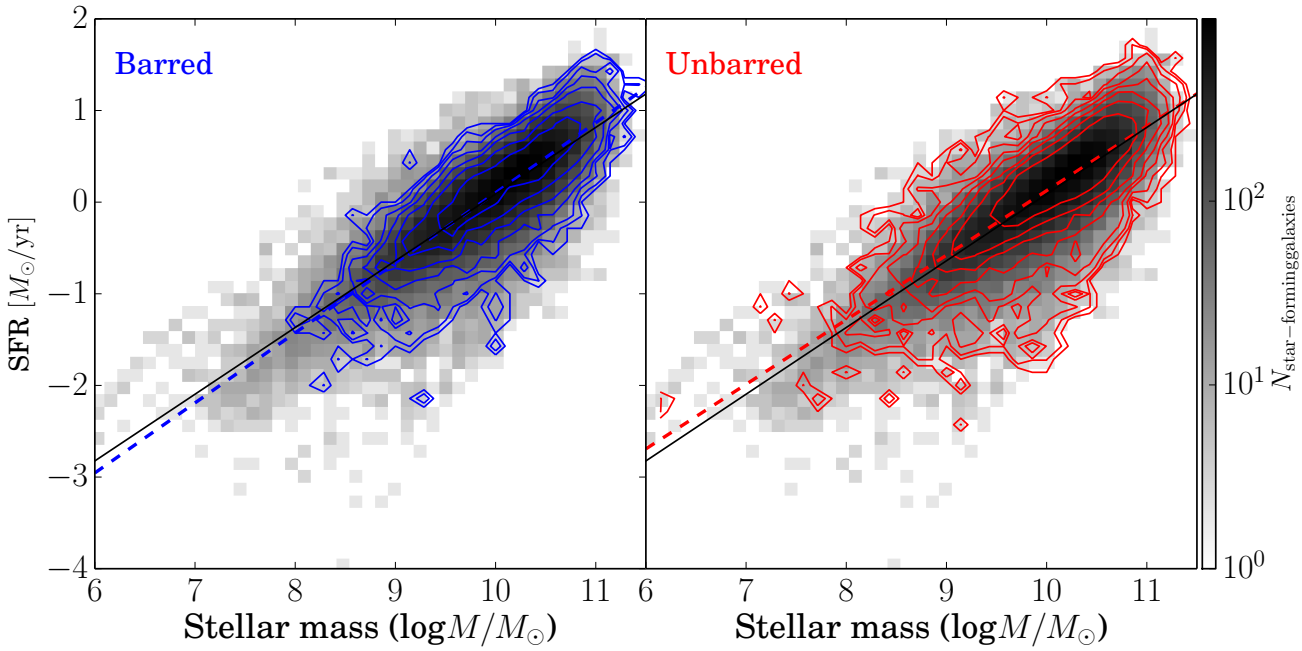

FIG. 3.— Stellar mass vs. star formation rate; grayscale colors are the distribution of all star-forming galaxies as in Figure 1. Left: blue contours show the distribution of barred galaxies ($p_{\mathrm{bar}} \geq 0.4$ for previously-identified disks) from GZ2. Right: red contours are the distribution of remaining disk galaxy population with no evidence for a strong bar ($p_{\mathrm{bar}} < 0.4$). Dotted lines show the weighted least-squares linear fit to the barred/unbarred population; the solid line is the fit to all star-forming galaxies.

These results confirm the trend in specific star formation rate seen by Darg et al. (2010b). We know that this is true at low redshift, but not at higher redshift. Rodighiero et al. (2011) show a significant increase at $1.5 < z < 2.5$, likely due to the *higher gas fraction* in galaxies at these redshifts. Also significant difference in disks at low/high redshift when using disk surface density instead of mass (Daddi et al. 2010). Elbaz et al. (2011) show that "compact" galaxies lie significantly off the SFR-MS using *Herschel* data. In the local Universe, green pea galaxies are the only objects that significantly exceed the main sequence, as evidenced by their sSFR (Cardamone et al. 2009).

Connection between galaxy structure and quenching efficiency - Omand et al. (2014) found a simple dependence on B/T for SDSS DR7 data.

Abramson et al. (2014) find that the sSFR in galactic disks is independent of mass.

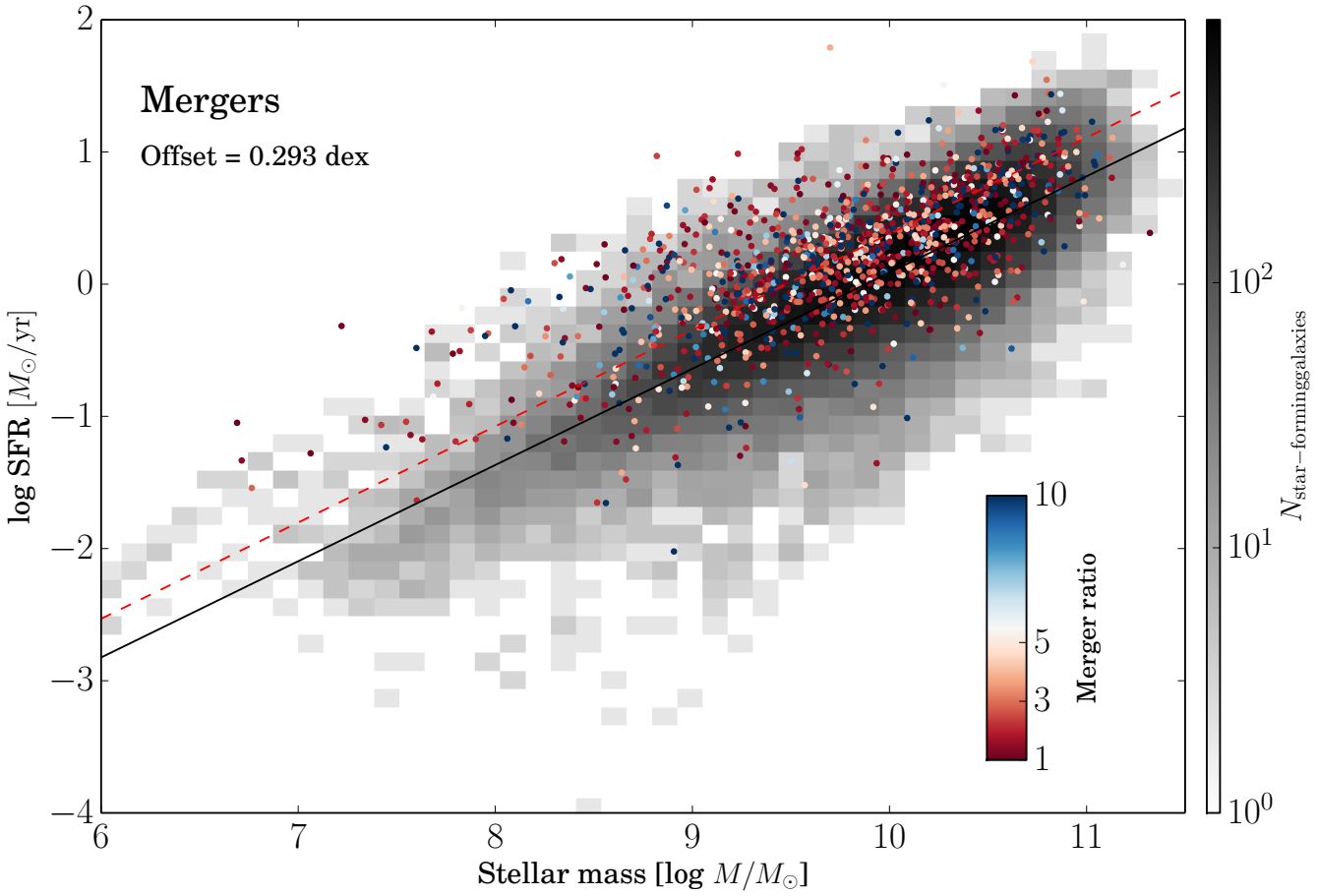

FIG. 4.— Stellar mass vs. star formation rate as in Figure 1. for 2,978 merging galaxies in GZ, as compared to the broader star-forming population. When fixing the slope of the star-forming main sequence and allowing the offset to vary, mergers have higher SFR of ~ 0.2 dex.

Check the mergers against the IR-derived star formation rates of Jarrett et al. (2013)?

The data in this paper are the result of the efforts of the Galaxy Zoo volunteers, without whom none of this work would be possible. Their efforts are individually acknowledged at http://authors.galaxyzoo.org. Please contact the authors to request access to research materials discussed in this paper.

We thank Rory Smith and Lucio Mayer for useful discussions. This research made use of TOPCAT, an interactive graphical viewer and editor for tabular data (Taylor 2005).

Funding for the SDSS and SDSS-II has been provided by the Alfred P. Sloan Foundation, the Participating Institutions, the National Science Foundation, the U.S. Department of Energy, the National Aeronautics and Space Administration, the Japanese Monbukagakusho, the Max Planck Society, and the Higher Education Funding Council for England. The SDSS website is http://www.sdss.org/.

The SDSS is managed by the Astrophysical Research Consortium for the Participating Institutions. The Participating Institutions are the American Museum of Natural History, Astrophysical Institute Potsdam, University of Basel, University of Cambridge, Case Western Reserve University, University of Chicago, Drexel University, Fermilab, the Institute for Advanced Study, the Japan Participation Group, Johns Hopkins University, the Joint Institute for Nuclear Astrophysics, the Kavli Institute for Particle Astrophysics and Cosmology, the Korean Scientist Group, the Chinese Academy of Sciences (LAMOST), Los Alamos National Laboratory, the Max-Planck-Institute for Astronomy (MPIA), the Max-Planck-Institute for Astrophysics (MPA), New Mexico State University, Ohio State University, University of Pittsburgh, University of Portsmouth, Princeton University, the United States Naval Observatory, and the University of Washington.

REFERENCES

Abazajian, K. N., Adelman-McCarthy, J. K., Agüeros, M. A., et al. 2009, ApJS, 182, 543
Abramson, L. E., Kelson, D. D., Dressler, A., et al. 2014, ArXiv e-prints, arXiv:1402.7076
Baldwin, J. A., Phillips, M. M., & Terlevich, R. 1981, PASP, 93, 5
Bouché, N., Dekel, A., Genzel, R., et al. 2010, ApJ, 718, 1001
Brinchmann, J., Charlot, S., White, S. D. M., et al. 2004, MNRAS, 351, 1151
Cardamone, C., Schawinski, K., Sarzi, M., et al. 2009, MNRAS, 399, 1191
Carpineti, A., Kaviraj, S., Darg, D., et al. 2012, MNRAS, 420, 2139
Casteels, K. R. V., Bamford, S. P., Skibba, R. A., et al. 2013, MNRAS, 429, 1051
Daddi, E., Elbaz, D., Walter, F., et al. 2010, ApJ, 714, L118
Darg, D. W., Kaviraj, S., Lintott, C. J., et al. 2010a, MNRAS, 401, 1043
—. 2010b, MNRAS, 401, 1552
Elbaz, D., Dickinson, M., Hwang, H. S., et al. 2011, A&A, 533, A119
Ellison, S. L., Nair, P., Patton, D. R., et al. 2011, MNRAS, 416, 2182
Hoyle, B., Masters, K. L., Nichol, R. C., et al. 2011, MNRAS, 415, 3627
Jarrett, T. H., Masci, F., Tsai, C. W., et al. 2013, AJ, 145, 6
Kauffmann, G., Heckman, T. M., White, S. D. M., et al. 2003a, MNRAS, 341, 33
Kauffmann, G., Heckman, T. M., Tremonti, C., et al. 2003b, MNRAS, 346, 1055
Lilly, S. J., Carollo, C. M., Pipino, A., Renzini, A., & Peng, Y. 2013, ApJ, 772, 119
Lintott, C., Schawinski, K., Bamford, S., et al. 2011, MNRAS, 410, 166
Lintott, C. J., Schawinski, K., Slosar, A., et al. 2008, MNRAS, 389, 1179
Masters, K. L., Nichol, R. C., Hoyle, B., et al. 2011, MNRAS, 411, 2026
Omand, C., Balogh, M., & Poggianti, B. 2014, ArXiv e-prints, arXiv:1402.3394
Peng, Y., Lilly, S. J., Renzini, A., & Carollo, C. M. 2014, ArXiv e-prints, arXiv:1406.7291
Peng, Y., & Maiolino, R. 2014, ArXiv e-prints, arXiv:1402.5964
Peng, Y.-j., Lilly, S. J., Renzini, A., & Carollo, M. 2012, ApJ, 757, 4
Peng, Y.-j., Lilly, S. J., Kovač, K., et al. 2010, ApJ, 721, 193
Rodighiero, G., Daddi, E., Baronchelli, I., et al. 2011, ApJ, 739, L40
Strauss, M. A., Weinberg, D. H., Lupton, R. H., et al. 2002, AJ, 124, 1810
Taylor, M. B. 2005, in Astronomical Society of the Pacific Conference Series, Vol. 347, Astronomical Data Analysis Software and Systems XIV, ed. P. Shopbell, M. Britton, & R. Ebert, 29
Willett, K. W., Lintott, C. J., Bamford, S. P., et al. 2013, MNRAS, 435, 2835
York, D. G., Adelman, J., Anderson, Jr., J. E., et al. 2000, AJ, 120, 1579